Advanced Visual Medicine: Techniques, Applications and Software

Simulation & Visualization for Surgery Planning

Stefan Zachow
Department of Visualization & Data Analysis
Medical Planning Group
Zuse Institute Berlin (ZIB) - Germany

Computer Assisted Medicine

Due to rapidly evolving medical imaging techniques *Visualization in Medicine* becomes more and more important

Besides mere *visualization* of medical data, there is an increasing demand for performing *modifications* or even *functional simulations* based on individual data for extended diagnosis and *therapy planning*

http://www.zib.de/visual/medical/projects

Outline

Generation of virtual 3D anatomy

- Geometric reconstruction from medical image data and visualization with amira®
- Statistical 3D shape models, i.e. anatomy including its variation

3D model based therapy planning

- Interactive modification (structure, properties, etc.)
- Numerical simulation (deformation, flow, pressure, etc.)

Virtual 3D Anatomy

Requirements

- **Morphology**
  boundaries of, and interfaces between anatomic structures of interest
- **Geometry**
  consistent, high quality surface meshes and volumetric grids (for planning and simulation)
- **Atlases**
  mean or representative shapes of anatomic structures including statistical shape variation

Virtual 3D Anatomy

From medical image data (CT, MRI, ...)

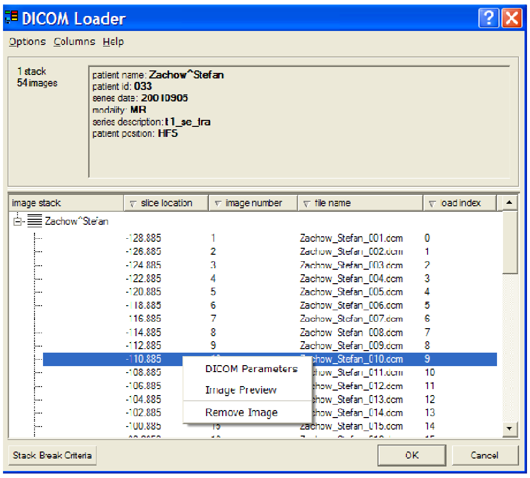

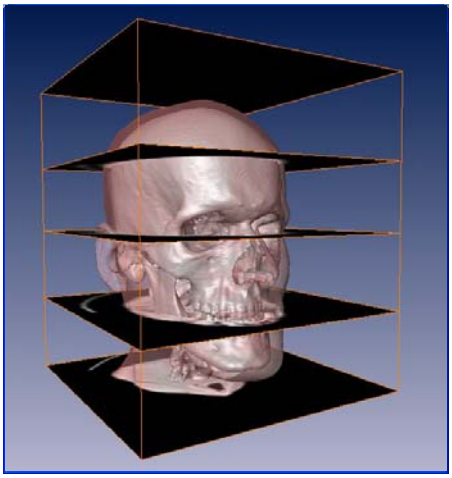

amira ®

Virtual 3D Anatomy

Consecutive slices of medical 2D images are converted into a 3D scalar field

- Scalars depend on the imaging modality, thus having a tissue related meaning
- Scalars can be visualized directly via volume rendering techniques using an appropriate mapping to display colors
- Scalars can be mapped to labels (single, multiple), which is called tissue classification or segmentation
- Boundaries of labeled regions can be computed and visualized using surface rendering techniques

Virtual 3D Anatomy

Visualization (Diagnostics)

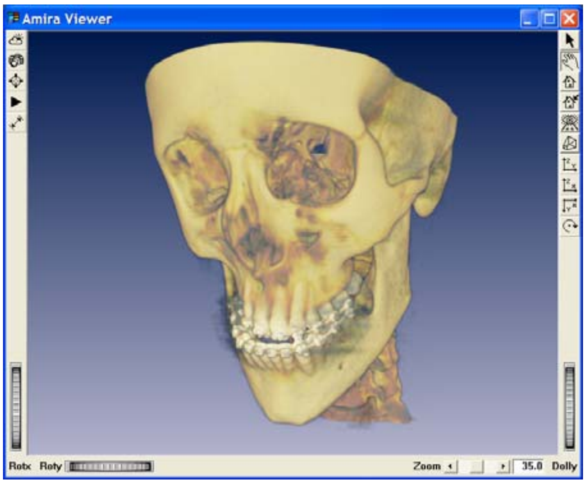

Volume Rendering

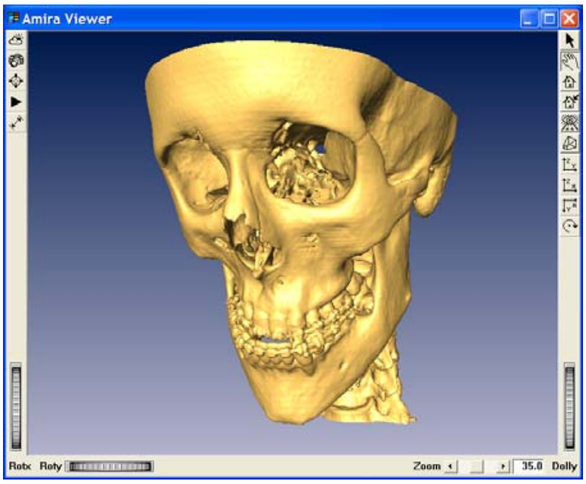

Iso-Surface (bone threshold)

Virtual 3D Anatomy

Segmentation of medical image data typically is a labor intensive process, highly depending on

- image quality (specificity, signal to noise ratio)
- image resolution (voxel size, number of slices)
- number of anatomic structures
- homogeneity of tissue structures
- separability of adjacent structures

Appropriate software tools are needed!

Virtual 3D Anatomy

Tissue Classification / Segmentation

- thresholding
- 2D/3D region growing
- lasso, brush, snakes
- intelligent scissors
- inter- / extrapolation
- morphological operators
- smoothing, denoising
- … to be improved !

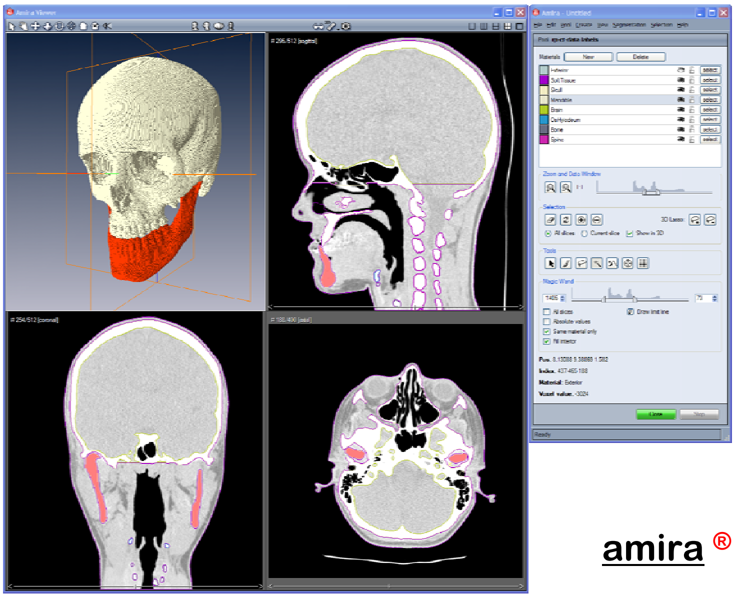

amira ®

Virtual 3D Anatomy

Tissue Boundaries / Surface Meshes

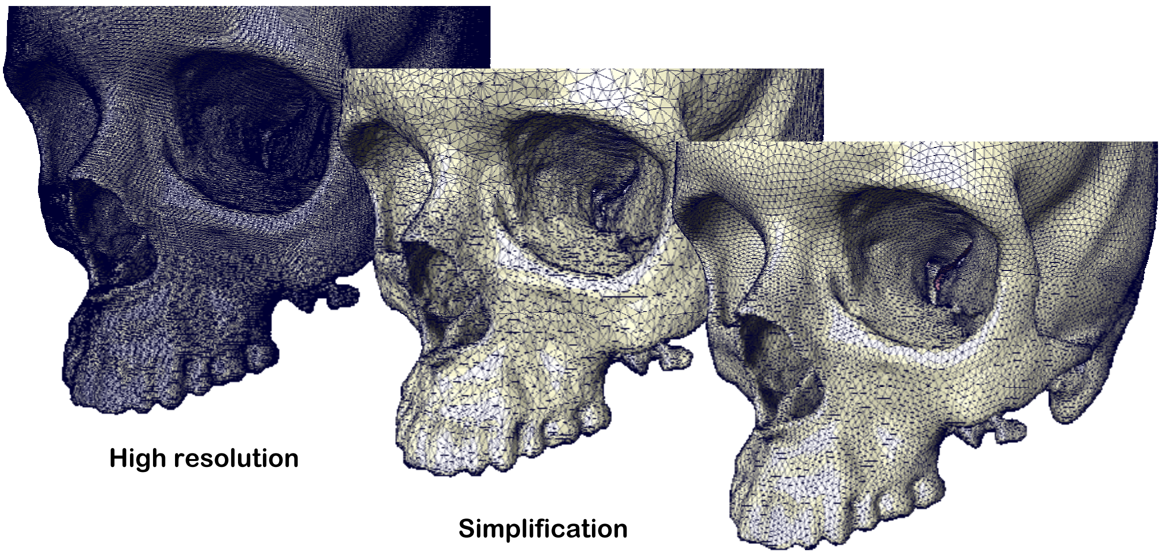

Virtual 3D Anatomy

Digital Anatomy

Surface meshes and volumetric grids for finite element analysis

- unstructured
- locally adaptive resolution
- controlled element quality

$$Quality = \frac{R_{inside}/R_{outside}}{(R_{inside}/R_{outside})_{ideal}}$$

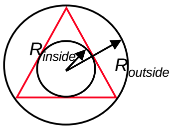

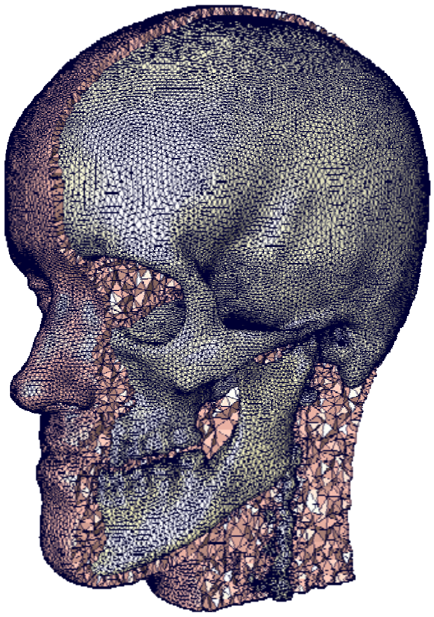

Virtual 3D Anatomy

Virtual Patient Models

- contain all relevant anatomic structures
- are a faithful and consistent reproduction of real anatomy
- can be further processed with software tools
- are the foundation for computer assisted therapy planning

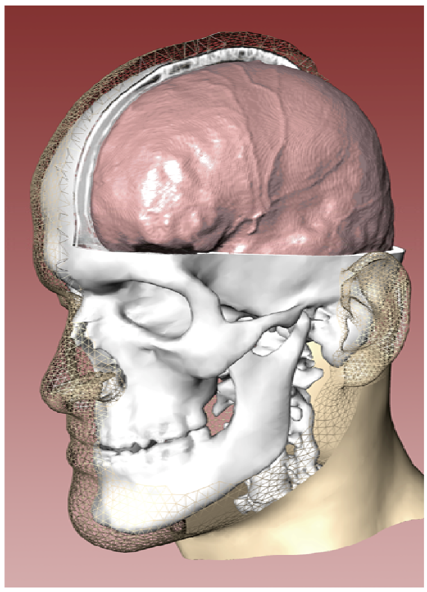

Virtual 3D Anatomy

Statistical Shape Models

- do represent not only a single shape of an anatomical structure but also its *shape variation* with regard to a set of similar structures
- are an extension of static reference anatomy (so called anatomical atlases)

… the "new anatomy" !

http://www.zib.de/lamecker/publications

Statistical Shape Models

Example: Mandible

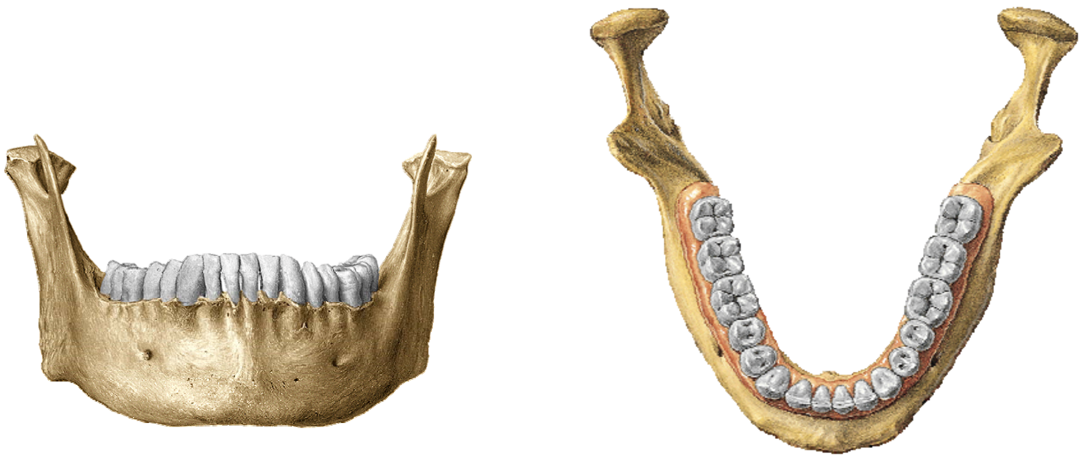

Härle et al.: *Atlas of Craniofacial Osteosynthesis*. Thieme (1999)

Mandibular Shapes are Manifold

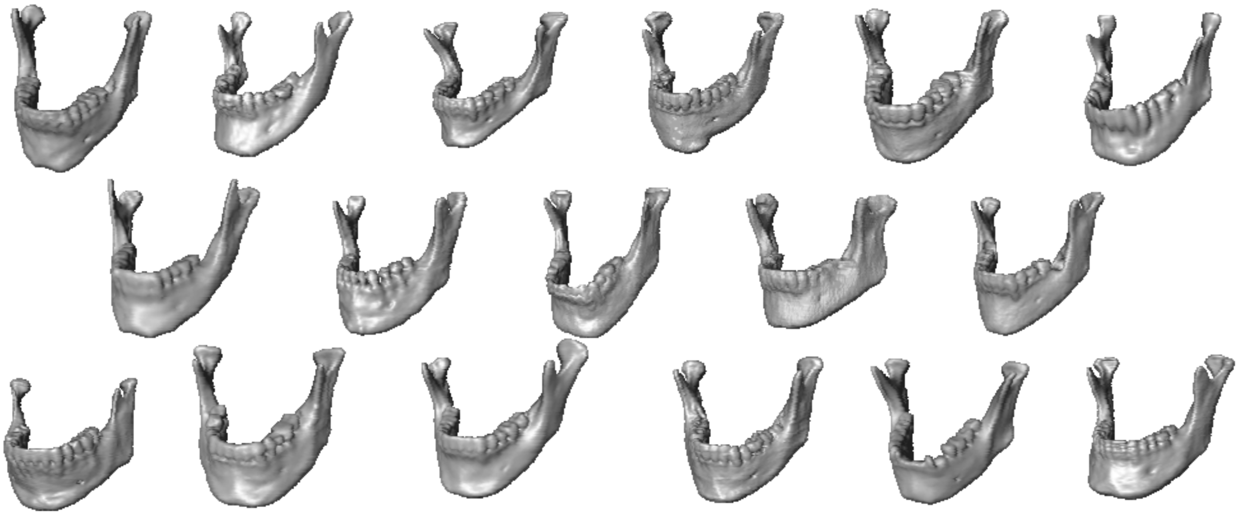

Consistent Shape Decomposition

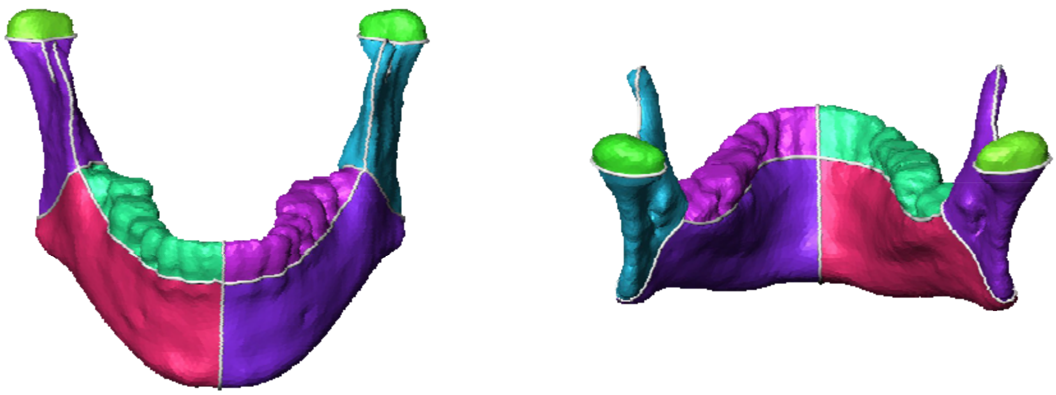

Statistical Shape Models

Reference Triangulation

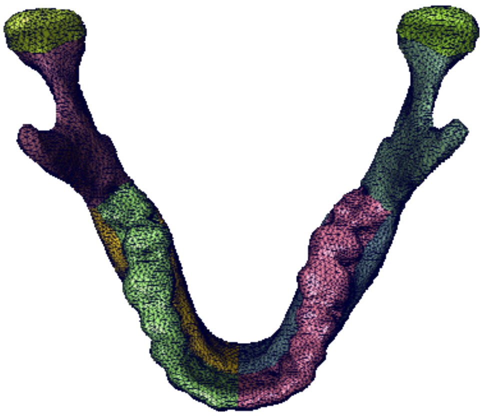

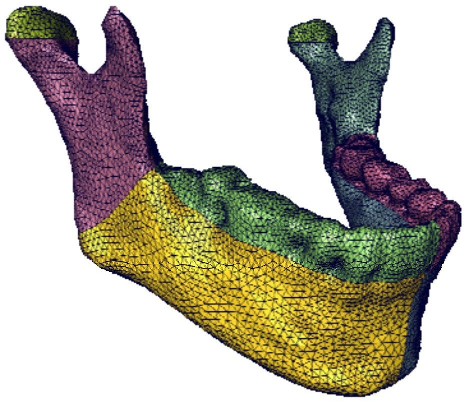

Statistical Shape Models

Consistent Surface Parameterization and Correspondence Mapping

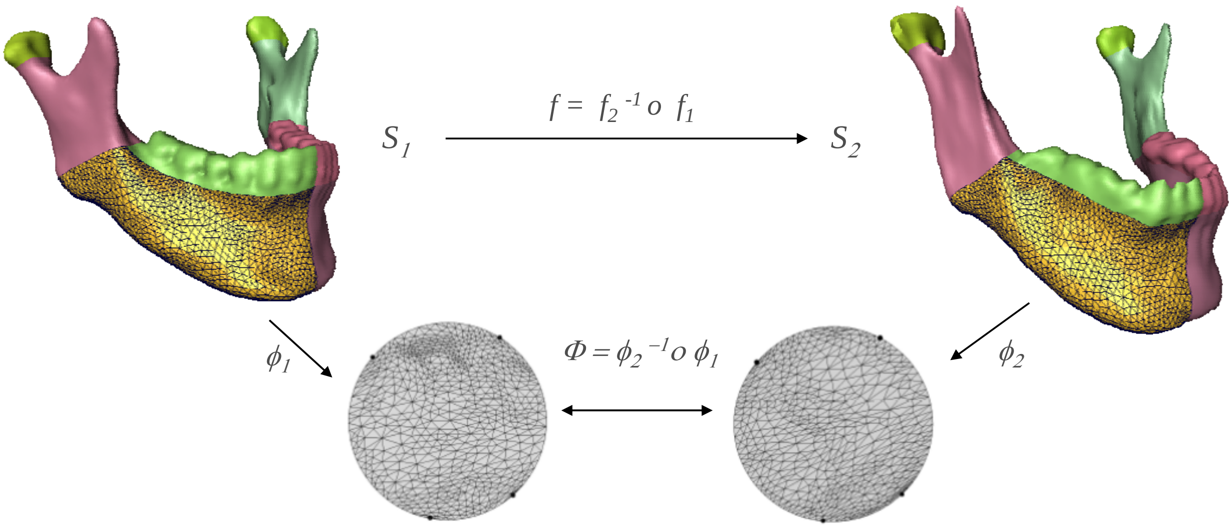

Statistical Shape Models

- correspondence maps → shape space $\mathbf{v}_k \in \mathbb{R}^{3m}$
  m = number of surface nodes
  k = 1,...,n with n = number of shapes
- principal component analysis on vectors $\mathbf{p}_k \in \mathbb{R}^{3m}$
  average shape
  eigenvectors of covariance matrix (modes of variation)
- statistical shape model $\mathcal{S}(\mathbf{b}, T) = T\left(\bar{\mathbf{v}} + \sum_{k=1}^{n} b_k \mathbf{p}_k\right)$
- essential degrees of freedom $n' \ll n$
  rigid-body / affine transformation T
  weights of modes of variation $b_k \in \mathbb{R}$

Statistical Shape Models

Averaging 3D Shapes

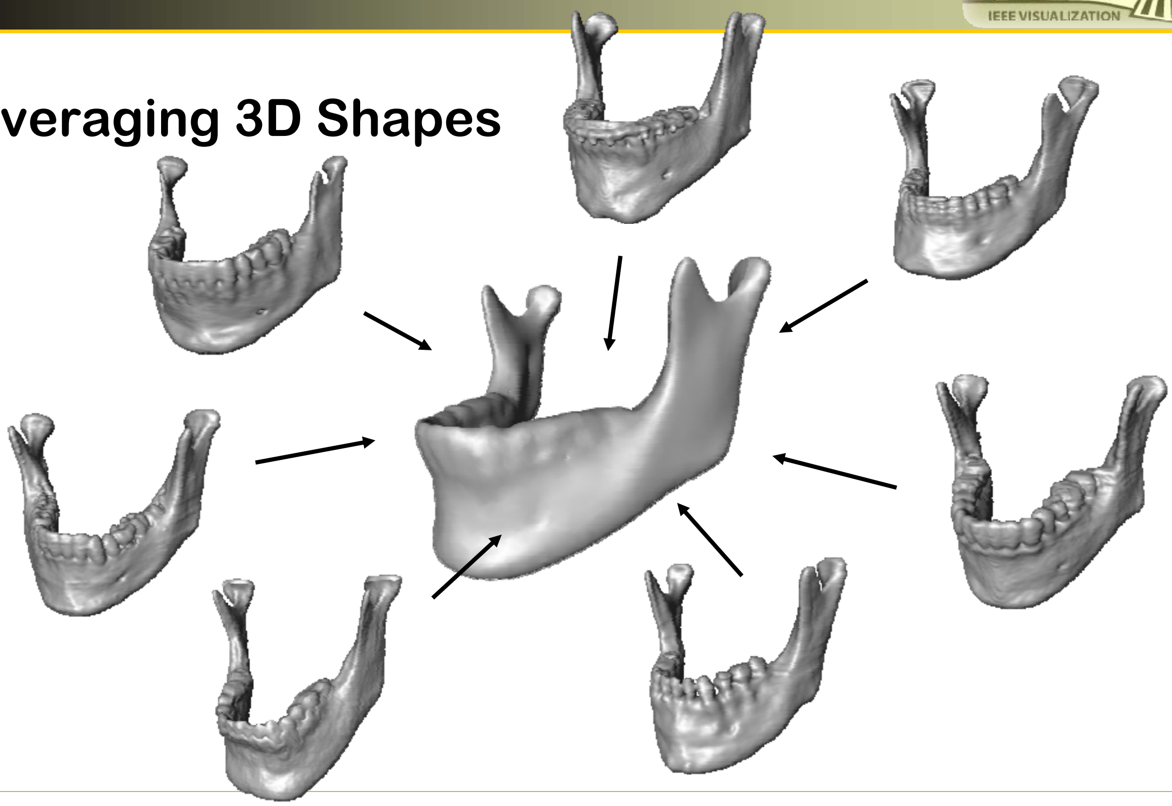

Statistical Shape Models

Characteristic Shape Variations

- the principal modes of variation are sorted according to their eigenvalues

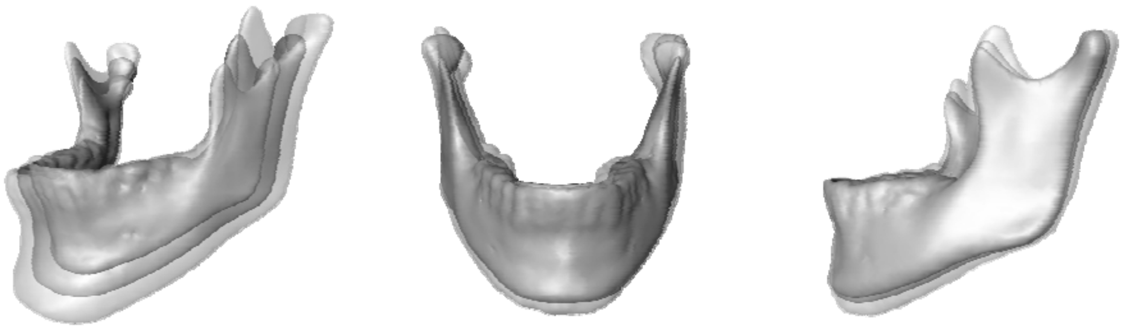

Statistical Shape Models

Example: Liver model of 50^{++} individuals

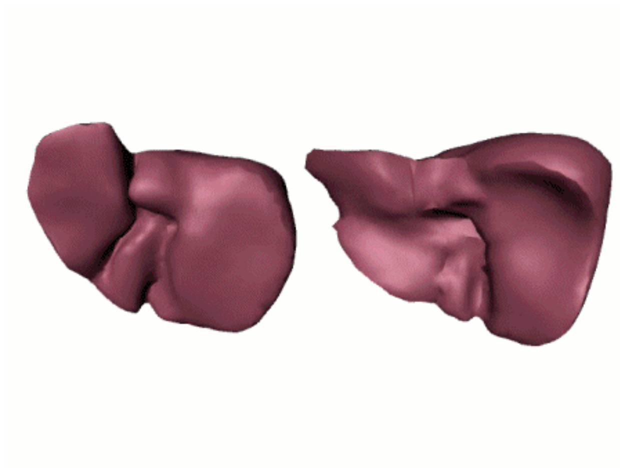

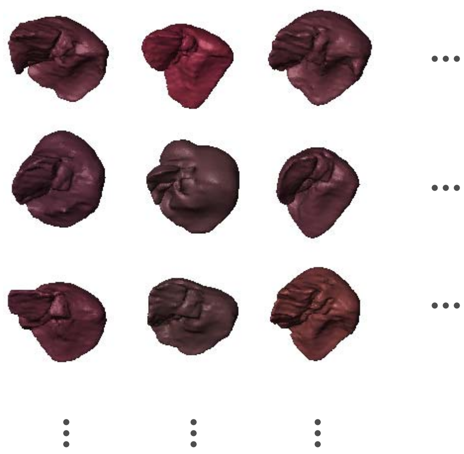

Statistical Shape Models

Averaged liver with first mode of variation

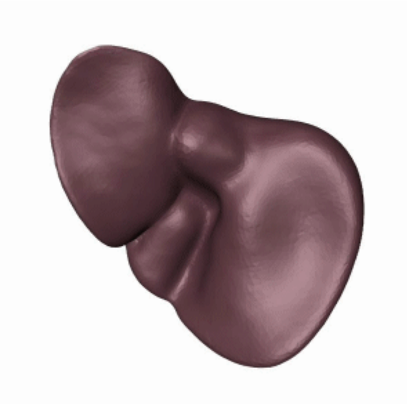

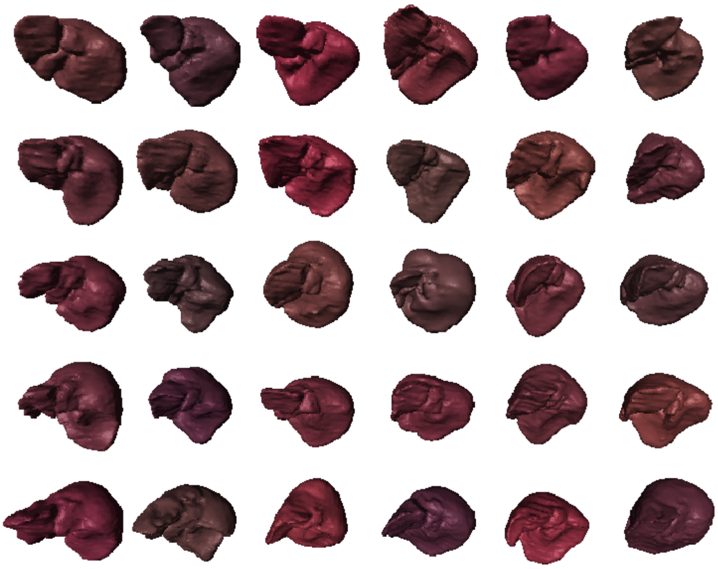

Statistical Shape Models

3D Model-based Segmentation of the Liver

- iterative adaptation process
- explicit profile model

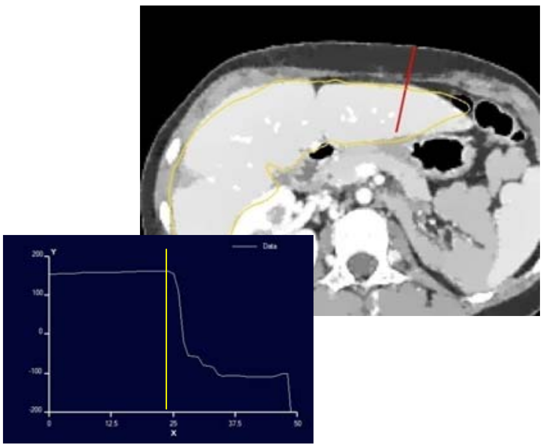

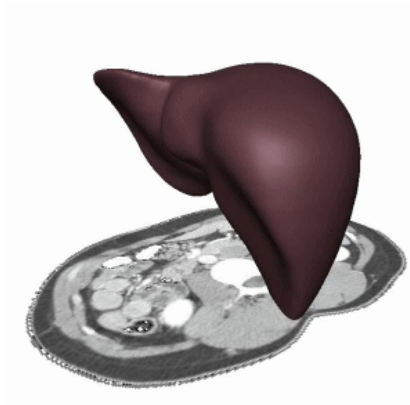

$$\min_{b_k, T} \left\| (\mathbf{v} + \Delta \mathbf{v}) - T\left(\overline{\mathbf{v}} + \sum_{k=1}^{n'} b_k \mathbf{p}_k \right) \right\|^2$$

Statistical Shape Models

Fully automatic segmentation of the liver from contrast enhanced CT-data

- Automatic initial positioning of the shape model according to anatomical landmarks
- Automatic initialization of intensity parameters via histogram analysis
- Adaptation of the statistical shape model (weighted combination of eigenmodes) acc. to image features
- Shape constrained free form deformation

D. Kainmüller, Th. Lange, H. Lamecker: *Shape constrained automatic segmentation of the liver based on a heuristic intensity model.* MICCAI Workshop on 3D Segmentation in the Clinic: A Grand Challenge, 2007

Statistical Shape Models

Fully automatic segmentation of the liver from contrast enhanced CT-data

- yellow: manual ref. segmentation
- blue: best possible adaptation of the statist. shape model
- red: free-form adaptation of the 3D shape model

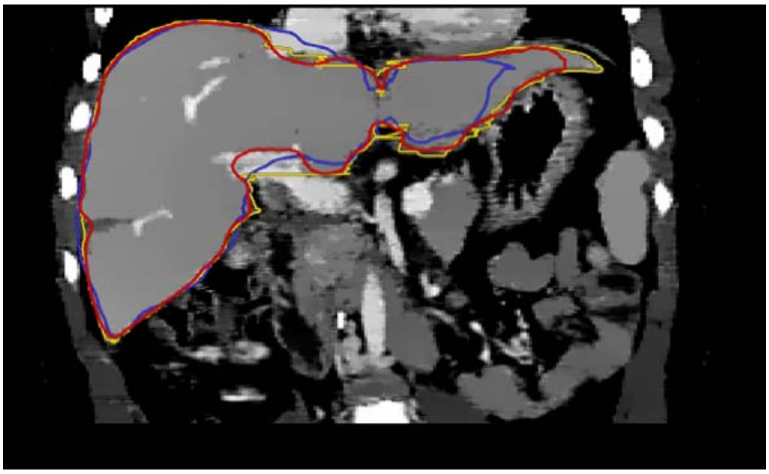

D. Kainmüller, Th. Lange, H. Lamecker: *Shape constrained automatic segmentation of the liver based on a heuristic intensity model.* MICCAI Workshop on 3D Segmentation in the Clinic: A Grand Challenge, 2007

Part II

3D Model-based Therapy Planning

Mental and technical preparation of complex medical interventions

- **Assessment**
  Type, location and extent of pathologies, functional (and esthetic) impairments, etc.
- **Strategy**
  Tools and methods, access paths, security margins, protection of vulnerable structures, etc.
- **Insight**
  Pre-interventional assessment of general outcome, effects on physiology, biomechanics, etc.

Therapy Planning

Applications

- Oncology - Regional Hyperthermia
- Maxillofacial Surgery – Osteotomy / Bone Relocation
- Craniofacial & Neurosurgery - Craniosynostosis
- Plastic and reconstructive surgery
- Ear, Nose and Throat Surgery - Rhinosurgery
- Orthopedic Surgery
- …

http://www.zib.de/visual/medical/projects

Therapy Planning in Oncology

Regional Hyperthermia

- Heating up tumor tissue above 42°C using radio waves without damaging surrounding tissue

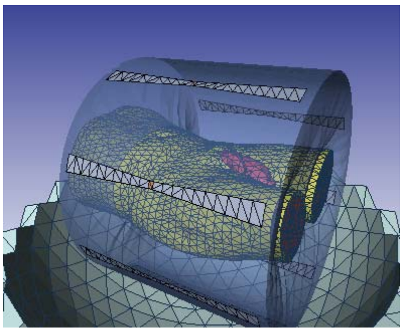

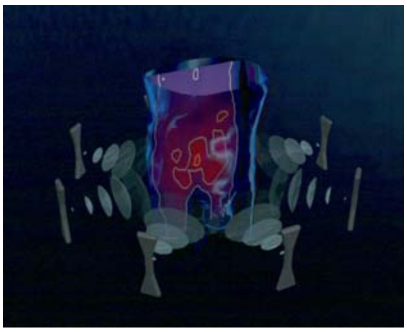

http://www.zib.de/visual/projects/hyperthermia/hyperthermialong.en.html

Therapy Planning in Oncology

Regional Hyperthermia

- An individual anatomic model of a tumor patient is generated
- The electro-magnetic field has to be computed according to the parameters of the applicator
- Energy distribution has to be computed within the patient model on basis of a heat transport equation as well as the specific absorption rates of tissues
- Applicator parameters, i.e. amplitudes and phases of the signals being sent to the antennas, are optimized in order to focus the heat within the tumor

Therapy Planning in Oncology

Regional Hyperthermia

- Field calculation: Maxwell‘s equations
- Temperature distribution: Heat transport equation

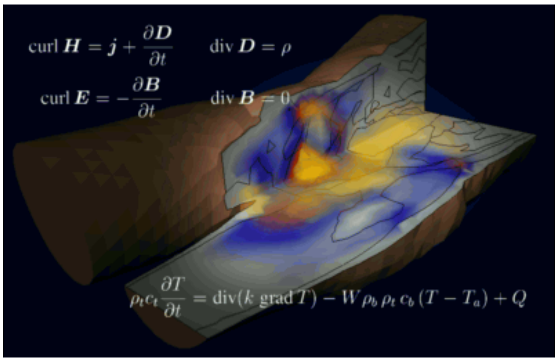

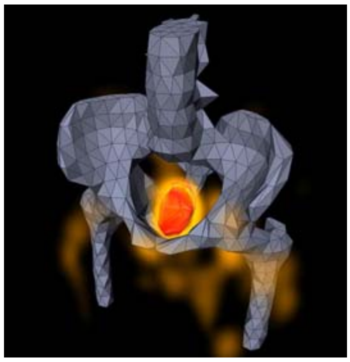

Therapy Planning in Maxillofacial Surgery

Maxillofacial Surgery

in cases of congenital pathologic development of the maxilla and/or mandible

http://www.zib.de/visual/projects/cas/caslong.en.html

Therapy Planning in Maxillofacial Surgery

Relocation of the Jaws

- Bone cuts (osteotomies) and
- Bone relocations to achieve
- Dental occlusion & facial harmony

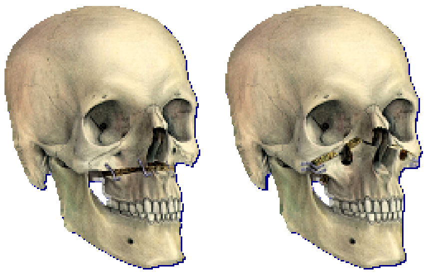

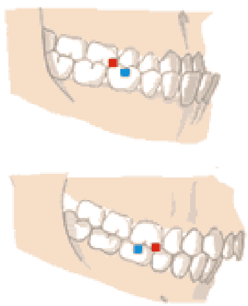

Härle et al: *Atlas of Craniomaxillofacial Osteosynthesis*. Thieme (1999)

Therapy Planning in Maxillofacial Surgery

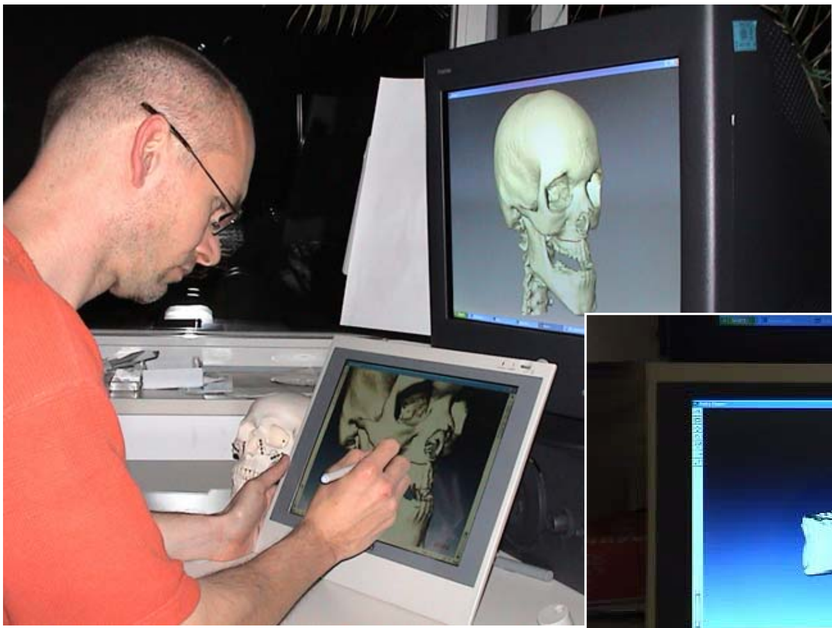

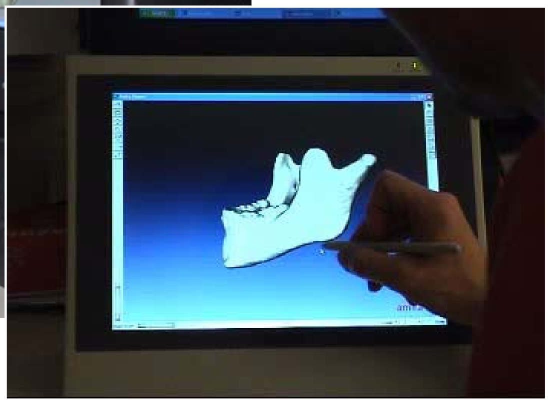

Computer-assisted osteotomy planning

Therapy Planning in Maxillofacial Surgery

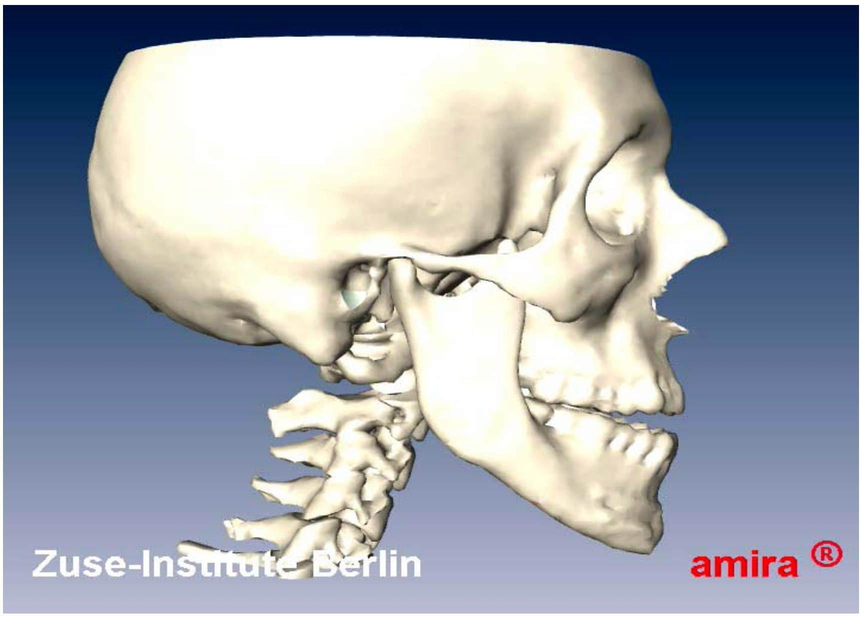

Example of a bimaxillary osteotomy

Therapy Planning in Maxillofacial Surgery

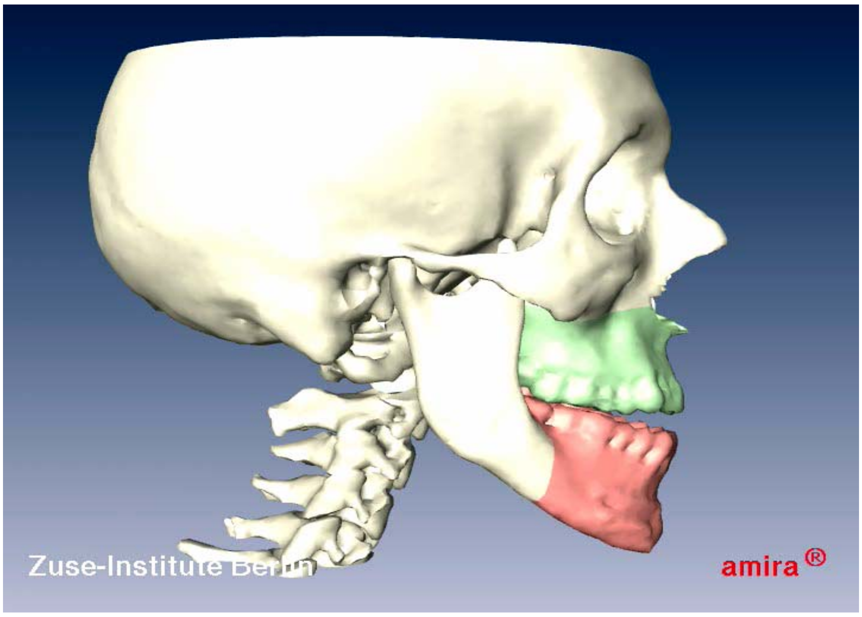

Bone relocation with soft tissue prediction

Therapy Planning in Maxillofacial Surgery

Soft Tissue Prediction

- based on the theory of 3D elasticity
- using a biomechanical tissue model
  (in the simplest case homogeneous and isotropic with Young's modulus E and Poisson ratio ν)

Stress-strain relationship

$$\sigma_{ij} \approx \frac{E}{1+\nu}\left(\varepsilon_{ij} + \frac{\nu}{1-2\nu}\varepsilon_{ll}\delta_{ij}\right)$$

$$\varepsilon_{ij} = \frac{1}{2}\left(u_{i,j} + u_{j,i}\right) + \ldots$$

Therapy Planning
in Maxillofacial Surgery

Minimization of internal deformation energy

$$W(\mathbf{u}) := \frac{1}{2}\int_{\Omega} \varepsilon : \sigma \, dV \longrightarrow min$$

Numerical solution of the Lamé-Navier equation

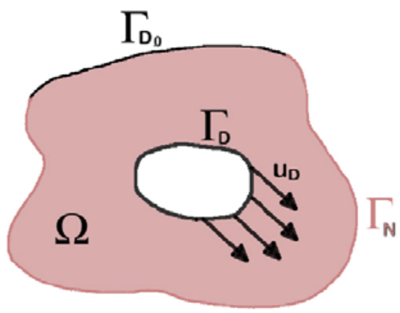

$$\frac{E}{2(1+\nu)}\left(\frac{1}{1-2\nu}\nabla(\nabla \cdot u(\mathbf{x})) + \Delta u(\mathbf{x})\right) = 0 \quad in\ \Omega$$

$$u(\mathbf{x}) = u_{D_0}(\mathbf{x}), \quad \mathbf{x} \in \Gamma_{D_0} \subset \partial\Omega$$

$$u(\mathbf{x}) = u_D(\mathbf{x}), \quad \mathbf{x} \in \Gamma_D \subset \partial\Omega$$

$$\sigma(\mathbf{x}) \cdot \mathbf{n} = 0, \quad \mathbf{x} \in \Gamma_N \subset \partial\Omega$$

Therapy Planning
in Maxillofacial Surgery

Osteotomy Planning with Soft Tissue Prediction

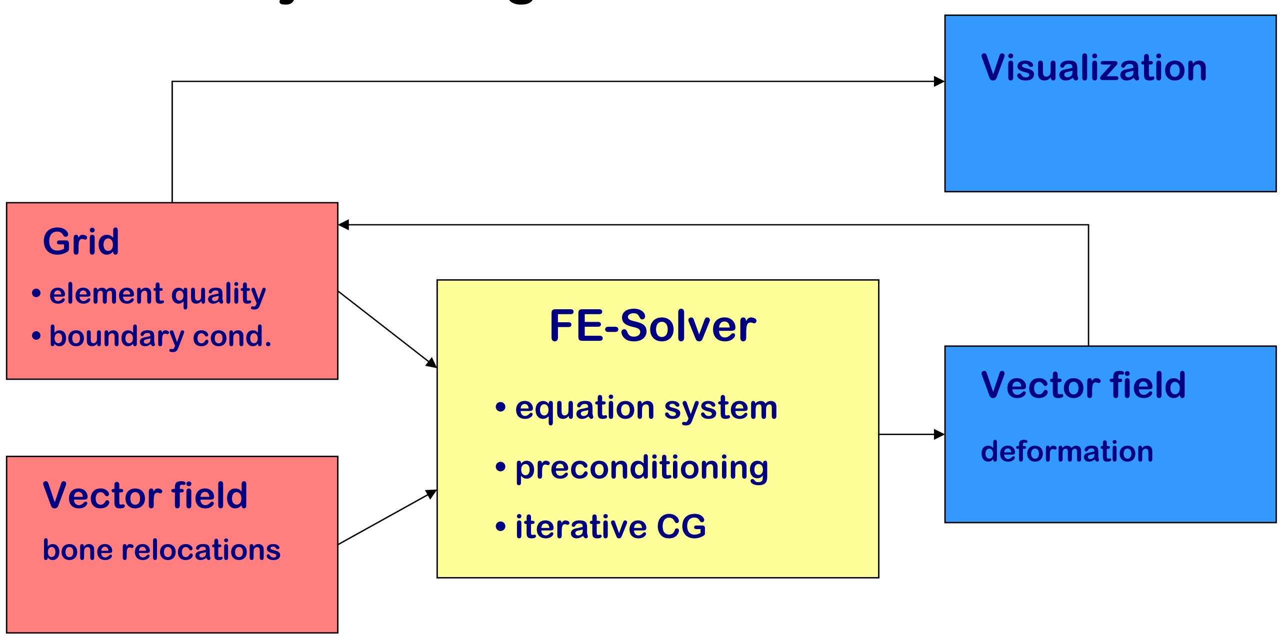

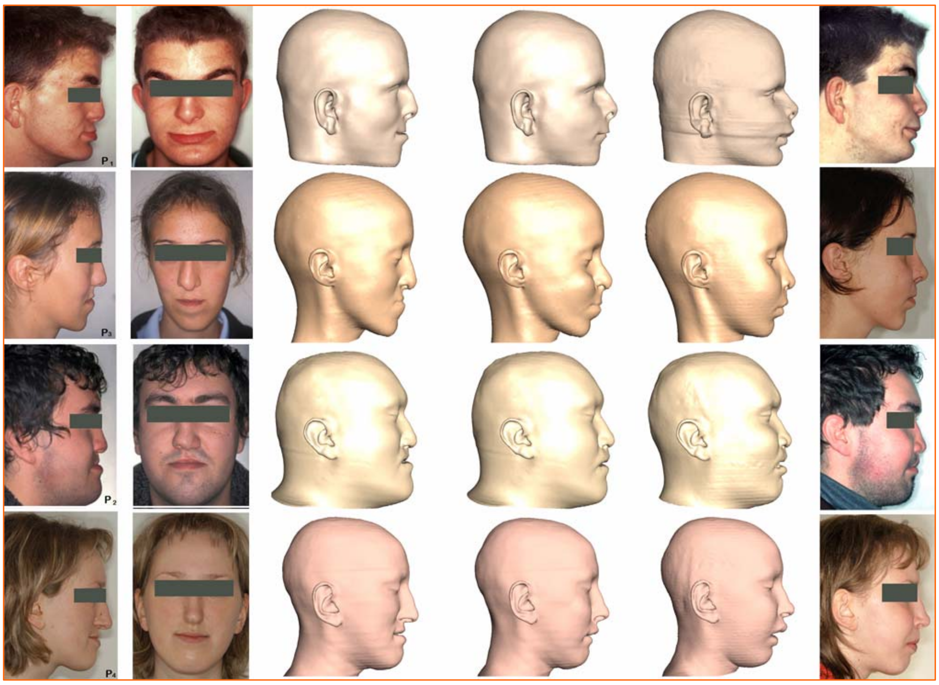

preoperative simulated postoperative

Severe Mandibular Dysplasia

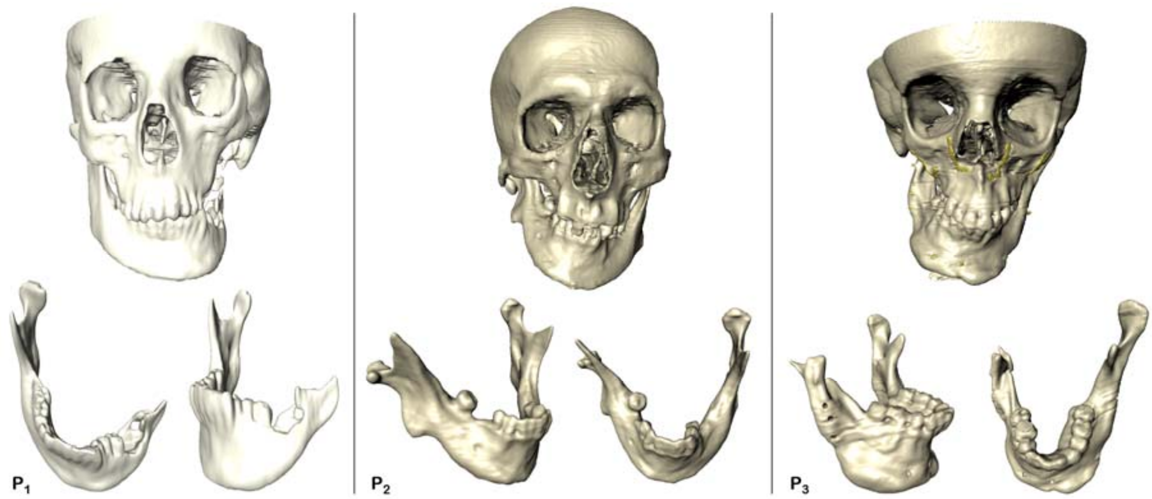

http://www.zib.de/visual/projects/mandiblerecon/mandiblerecon.frameset.en.html

Therapy Planning in Maxillofacial Surgery

Severe Mandibular Dysplasia

- due to tumor related bone resections or craniofacial microsomia
- Reconstruction cannot be guided by the symmetry of anatomical structures
- Either autologous bone grafts or implants are used for reconstruction
- A statistical shape model of a normally developed mandible is used as a reconstruction template

Therapy Planning in Maxillofacial Surgery

Partial Reconstruction of Bone Structures

- Adaptation of a statistical shape model of a normally developed mandible to unaffected structures

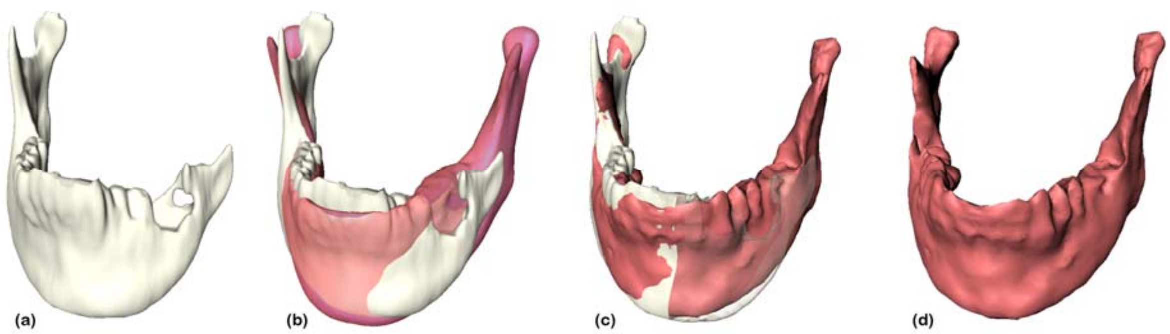

$$d_{\mathrm{rms}}(\mathcal{S}(\mathbf{b},T),\mathcal{S}') = \sqrt{\frac{1}{|\mathcal{S}|+|\mathcal{S}'|}\left(\int_{\mathbf{x}\in\mathcal{S}} d(\mathbf{x},\mathcal{S}')^2 d\mathcal{S} + \int_{\mathbf{x}\in\mathcal{S}'} d(\mathbf{x},\mathcal{S})^2 d\mathcal{S}\right)}.$$

Therapy Planning in Cranio-Neurosurgery

Surgical Correction of Skull Deformities

- Prematurely ossified cranial sutures in infants lead to skull deformities within the growth process
- Surgical correction is necessary to prevent functional impairment of the brain and to improve a patient’s appearance
- A preoperative planning method of reshaping the cranium with the help of a statistical shape model has been developed

http://www.zib.de/visual/projects/craniosynos/craniosynos.frameset.en.html

Therapy Planning in Cranio-Neurosurgery

Surgical Correction of Skull Deformities

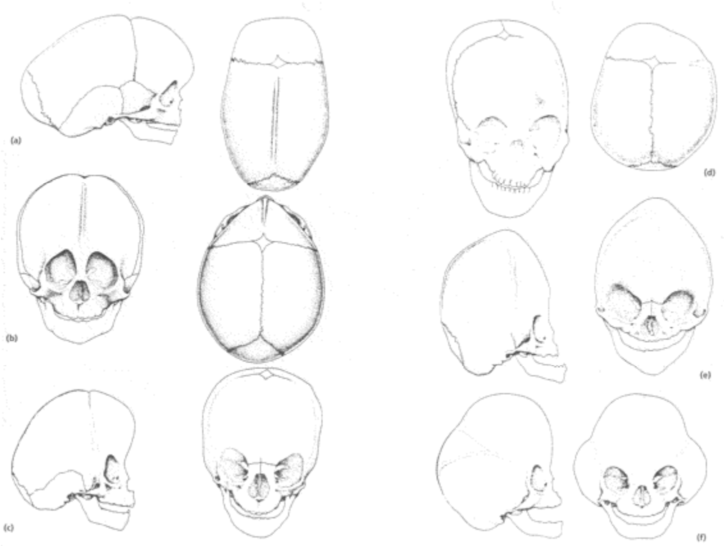

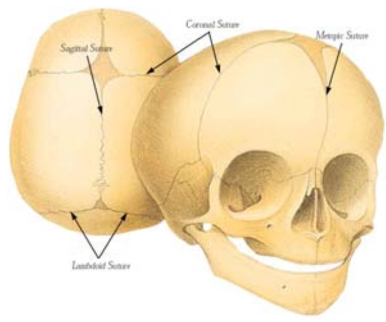

Thompson DN, Hayward RD. Craniosynostosis- pathophysiology, clinical presentation, and investigation.
In: Choux M, Di Rocco C, Hockley A, Walker M (Hrsg.): Pediatric Neurosurgery. Curchill Livingstone, London 1999, 276.

Surgical Correction of Skull Deformities

- Fragmentation, reshaping and reorganisation of cranial bone structures
- No target specification - aesthetic result is difficult to predict

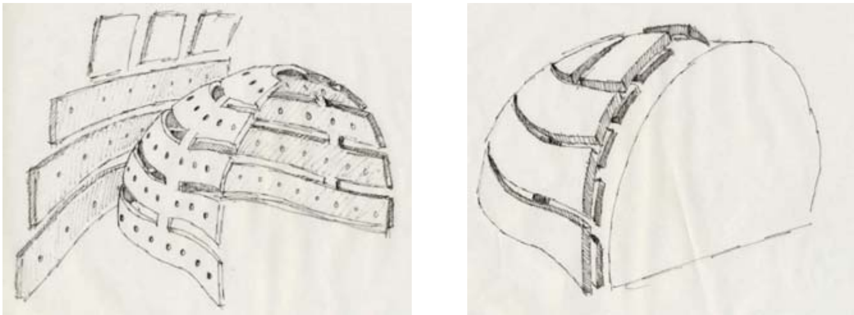

H. Haberl, 2002

A Statistical Shape Model of the Skull

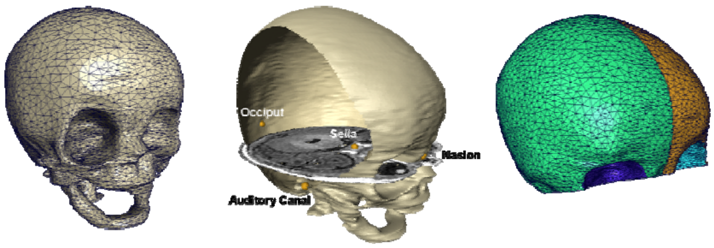

MRI data of 21 patients

age: 3 to 10 months

male/female

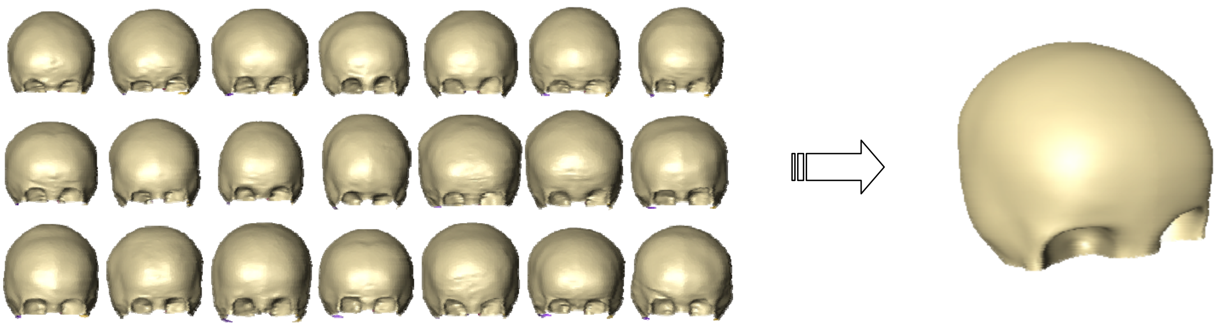

Clinical Case

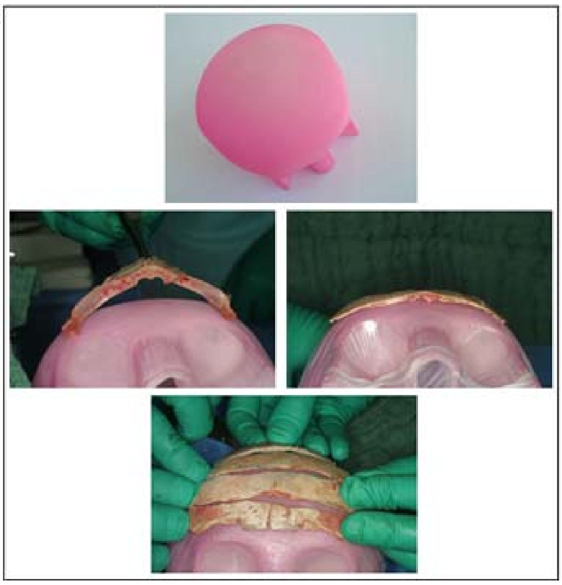

Individually manufactured template based on the adapted 3D shape model
for surgical reformation of the frontal skull bone (Haberl, Klein – Charité Berlin)

Orbital Wall Fractures

Enophthalmism

blow out fracture

orbital floor reconstruction

Postoperative result

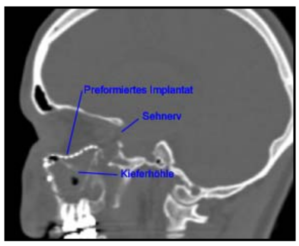

Postoperative assessment

http://www.zib.de/visual/projects/orbita/orbitalong.en.html

Therapy Planning in Orbit-Surgery

Mirroring of the Bony Orbit

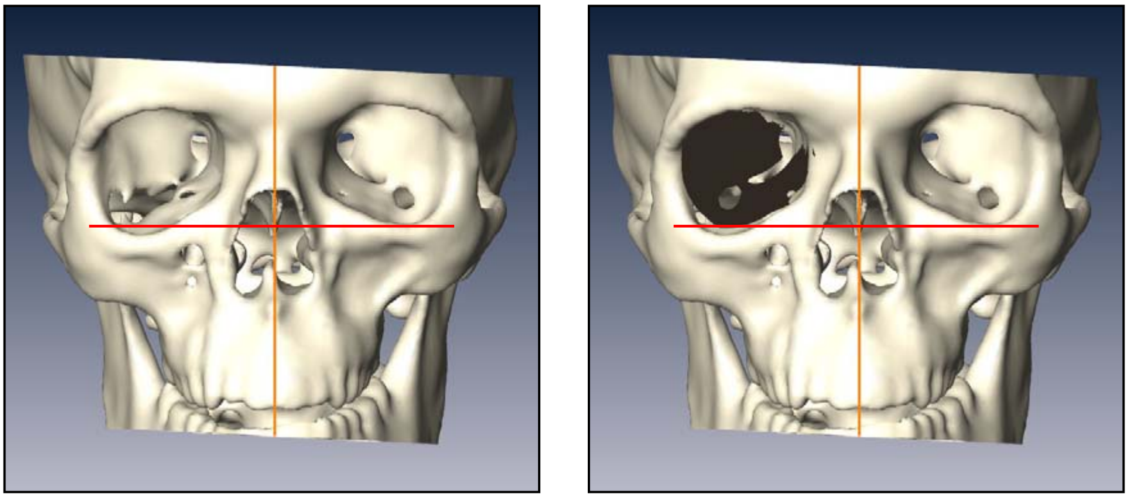

Planning in Cooperation with Dr. Kontio, Helsinki

Therapy Planning in Orbit-Surgery

Elevation of the Zygomatic Bone

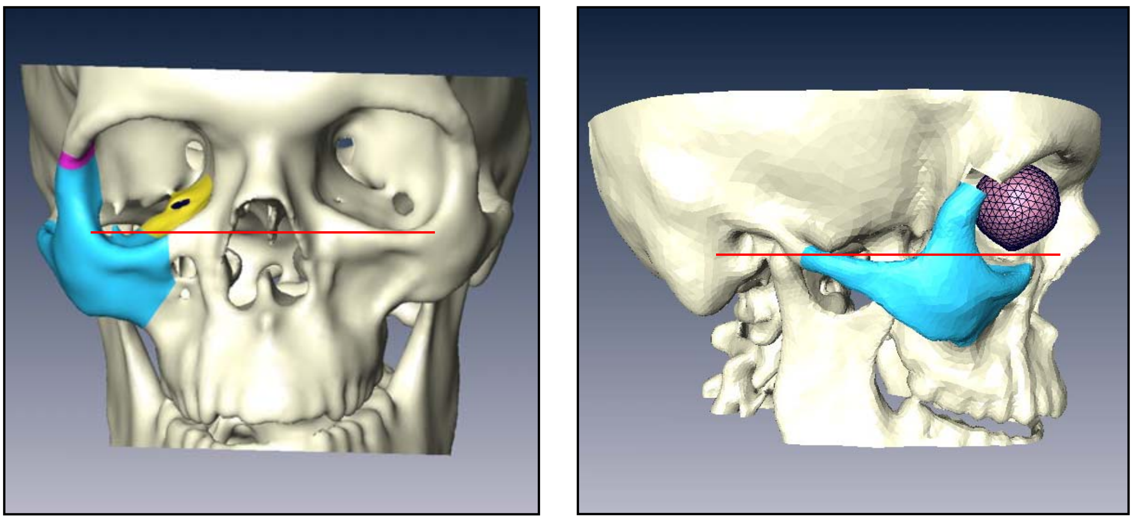

Elevation of the Zygomatic Bone

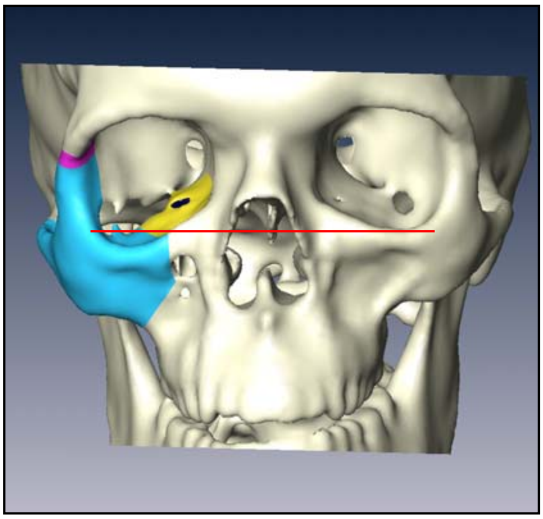
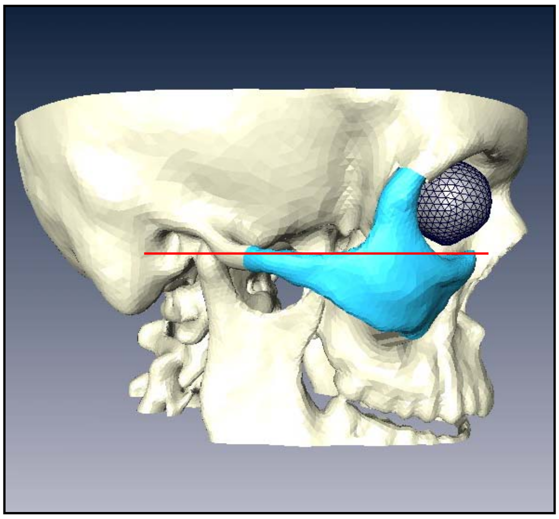

Elevation of the Eye Ball

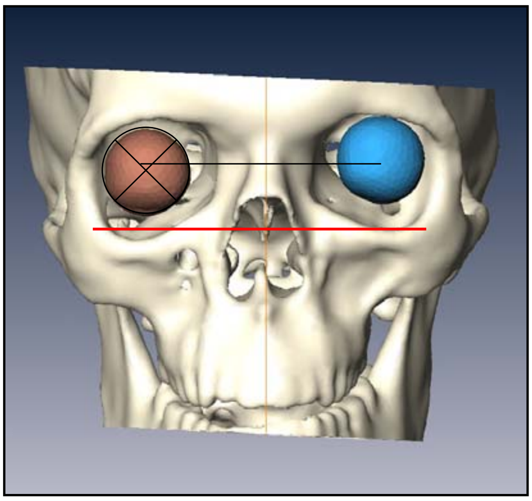
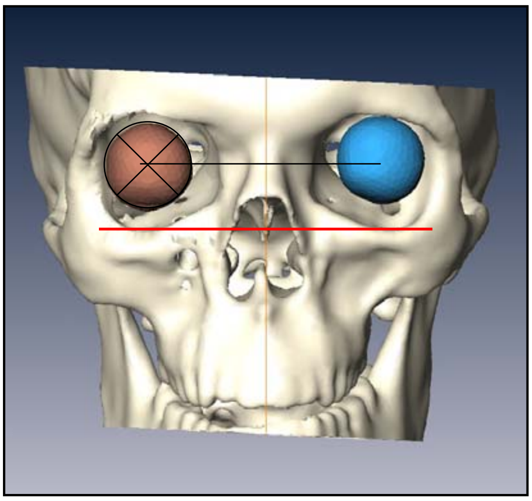

A Statistical Shape Model of the Orbit

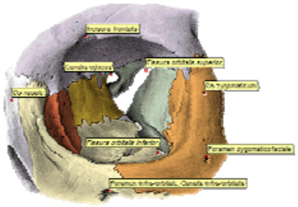

Anatomical regions of the orbit [Sobotta]

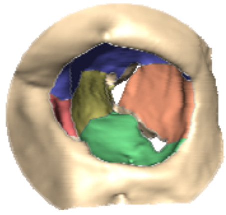

3D shape model of the human orbit

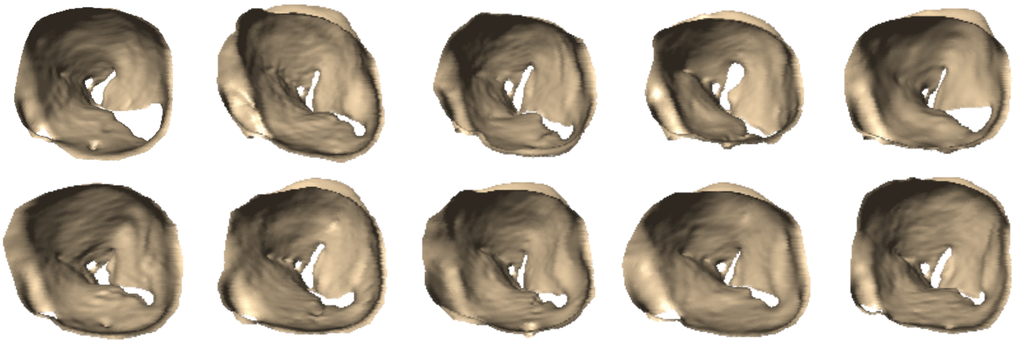

Therapy Planning
in Orbit-Surgery

Template for Custom Implant Design

	mean	first mode of variation (min/max)	
statistical model	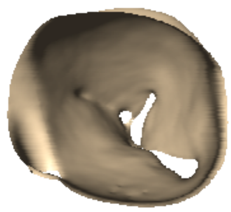	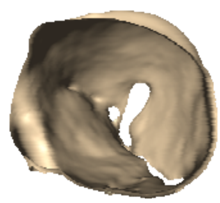	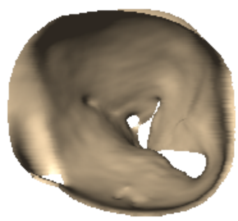
rapid prototyping			

Cooperation with Dr. Noser, AO Development Institute, Davos, Switzerland

Esthetics & Function

http://www.zib.de/visual/projects/nose/noselong.en.html

Function of the Nose

- Breathing - Smelling
- Cleaning the air
- Conditioning the air to body temperature
- Humidification

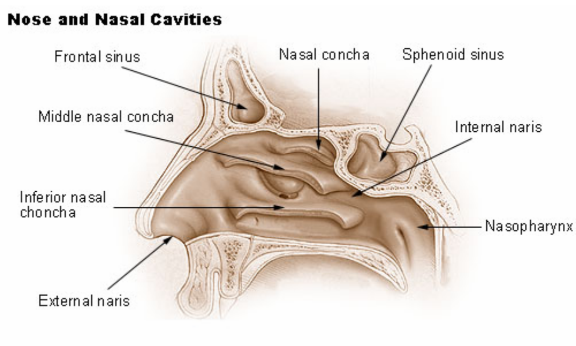

Surgical correction might be indicated

in cases where the function is disturbed, e.g. due to any obstruction or deformity.

Therapy Planning in Rhinosurgery

Dysfunction of the Nose

- Septal deviation
- Deformities of the external nose
- Paranasal sinusitis, nasal polyps

Therapy Planning in Rhinosurgery

Understanding Nasal Airflow

- Characterization of typical airflow phenomena
- Analysis of the correlation between shape and function of the nose
- Individualized therapy planning of rhinosurgery under consideration of *regular* nasal air flow

Understanding Nasal Airflow

Due to the complexity and the anatomical inaccessibility of the nasal cavities, as well as the limited availability of meaningful measuring methods

Modeling and simulation of nasal airflow via Computational Fluid Dynamics (CFD)

A Reference Model of the Nasal Airways

- Helical CT scan (64-slice) of a volunteer
- Local administration of a decongestant (xylometazoline)
- Systemic application of methylprednisolon

A Reference Model of the Nasal Airways

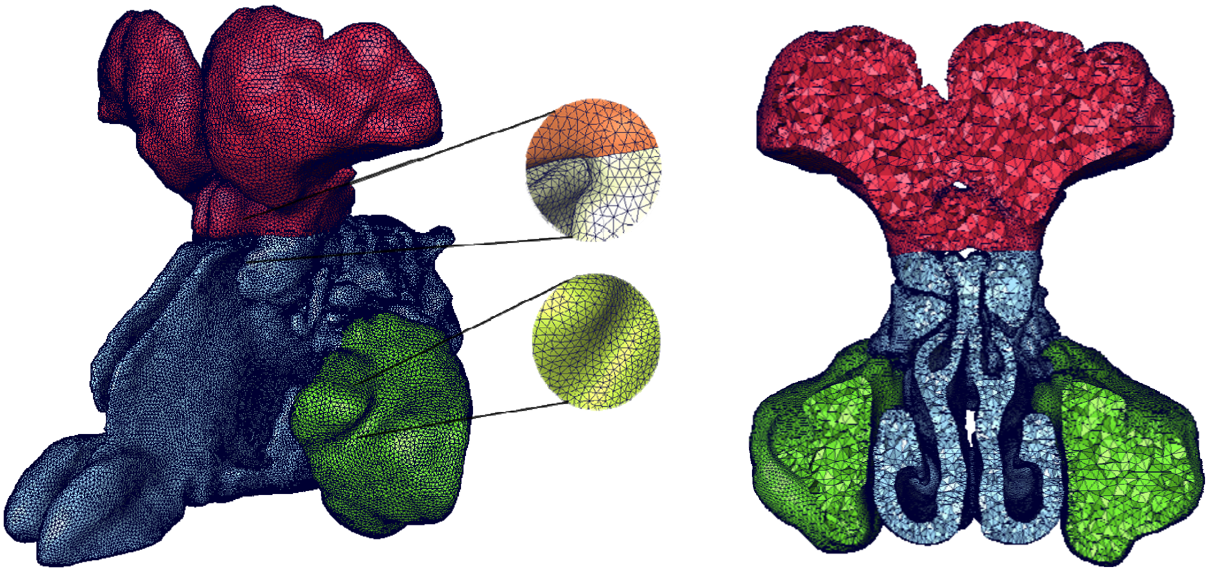

Upper Respiratory Tract and Inflow Region

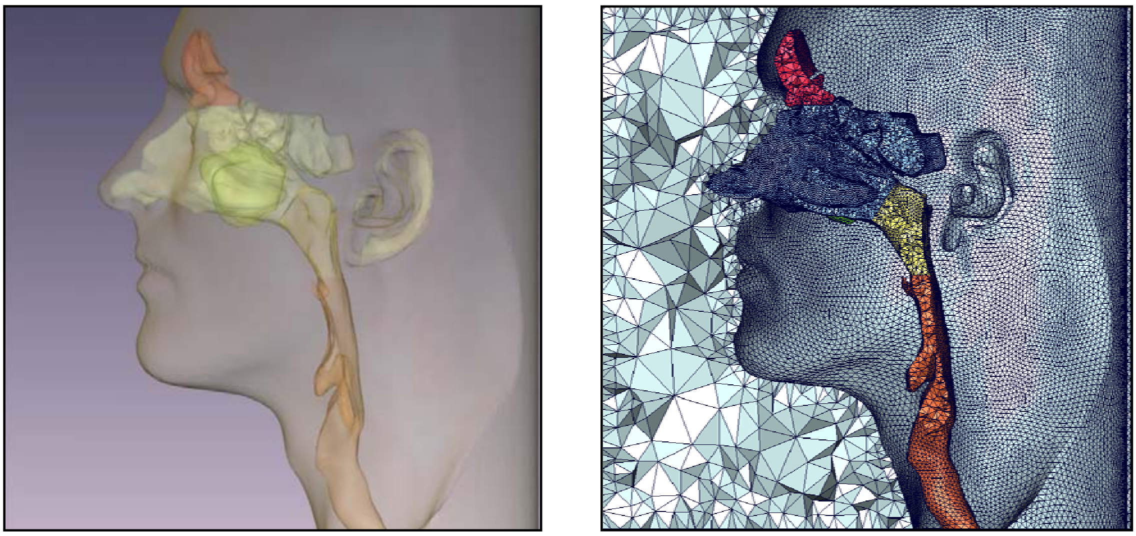

Therapy Planning in Rhinosurgery

Boundary conditions

Walls (mucosa)

- smooth
- flow involved friction

Air

- isothermal, incompressible
- density 1.185 kg/m^3
- dynamic viscosity 1.831 e^{-5} kg/m·s
- temperature 25 °C
- ambient pressure (absolute) 101325 Pa

Therapy Planning in Rhinosurgery

Boundary conditions

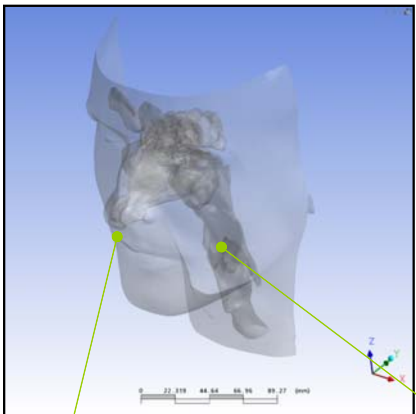

Outlet: trachea

Nostril 0 Pa

Steady state

- Outlet pressure = -150 Pa

Transient flow

- Time dep. pressure: Active Anterior Rhinomanometry (AAR)

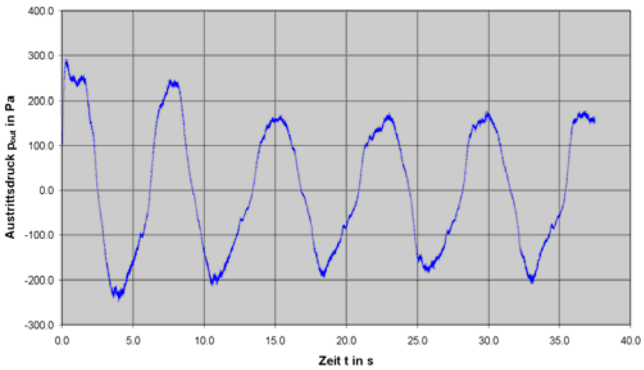

Computational Fluid Dynamics

- Conservation of mass

$$\frac{\partial\rho}{\partial t}+\frac{\partial(\rho u_i)}{\partial x_i}=0$$

- Conservation of momentum

$$\frac{\partial(\rho u_i)}{\partial t}+\frac{\partial(\rho u_i u_j)}{\partial x_j}=-\frac{\partial p}{\partial x_i}+\frac{\partial}{\partial x_j}\left(\mu\left(\frac{\partial u_i}{\partial x_j}+\frac{\partial u_j}{\partial x_i}-\frac{2}{3}\delta_{ij}\frac{\partial u_k}{\partial x_k}\right)\right)+f_i$$

- Conservation of energy

$$\frac{\partial(\rho E)}{\partial t}+\frac{\partial(\rho u_j E)}{\partial x_j}=-\frac{\partial(p u_j)}{\partial x_j}+\frac{\partial}{\partial x_j}\left(\lambda\frac{\partial T}{\partial x_j}\right)+\frac{\partial(u_i\tau_{ij})}{\partial x_j}+S_E$$

Therapy Planning
in Rhinosurgery

Computational Fluid Dynamics

- Transport equations

(Reynolds-averaged) Navier-Stokes PDE

$$\underbrace{\frac{\partial}{\partial t}(\rho\Phi)}_{\text{time alteration rate}}+\underbrace{v_j\frac{\partial}{\partial x_j}(\rho\Phi)}_{\text{convective transport}}=\underbrace{\Gamma_\Phi\frac{\partial^2\Phi}{\partial x_j^2}}_{\text{diffusive transport}}+\underbrace{S_\Phi}_{\text{production}}$$

Numerical solution of the averaged conservation equations (velocity and pressure field)

Ansys CFX ®

Therapy Planning in Rhinosurgery

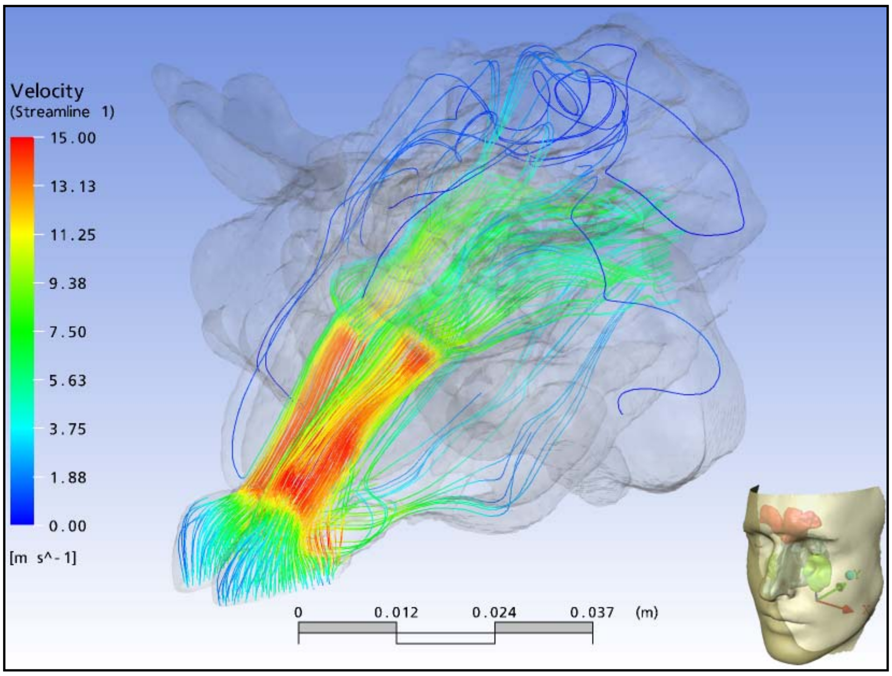

Visualization of inspiratory flow up to 16 m/s under laminar and turbulent conditions

Therapy Planning in Rhinosurgery

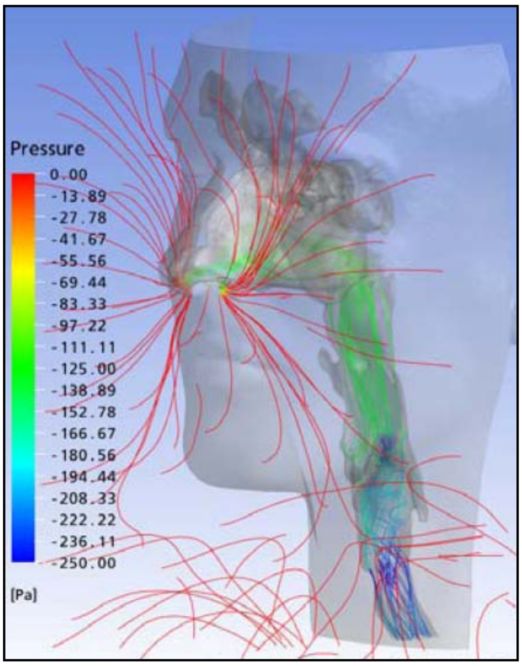

inhalation

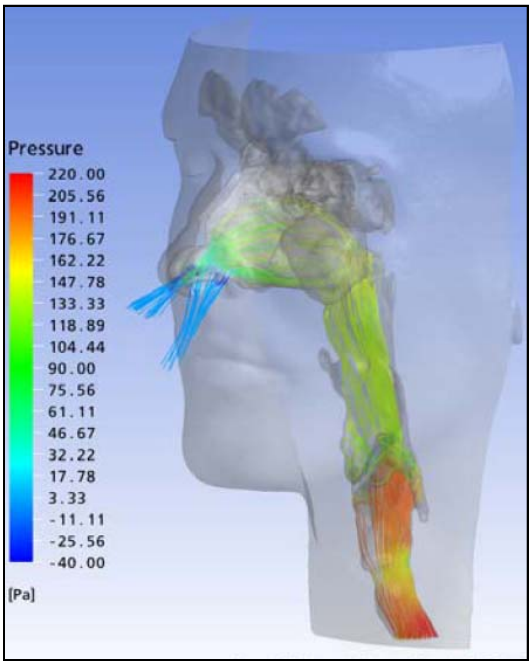

exhalation

Therapy Planning in Rhinosurgery

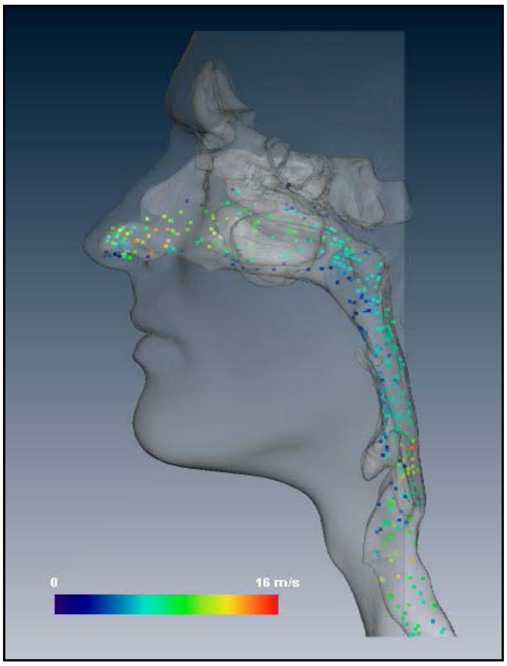

inhalation

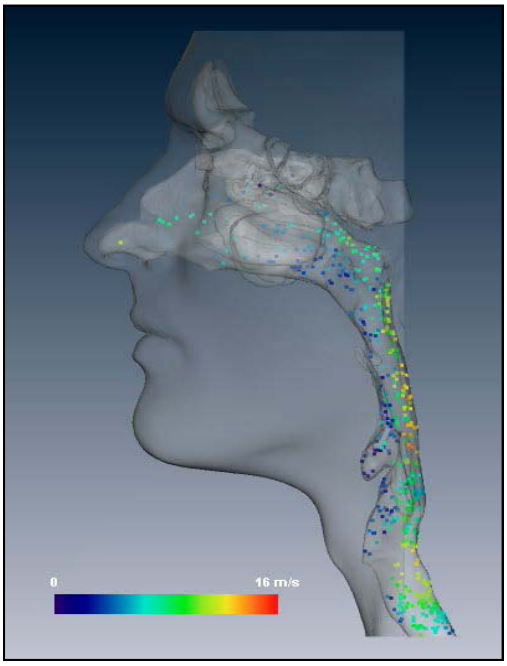

exhalation

Therapy Planning in Rhinosurgery

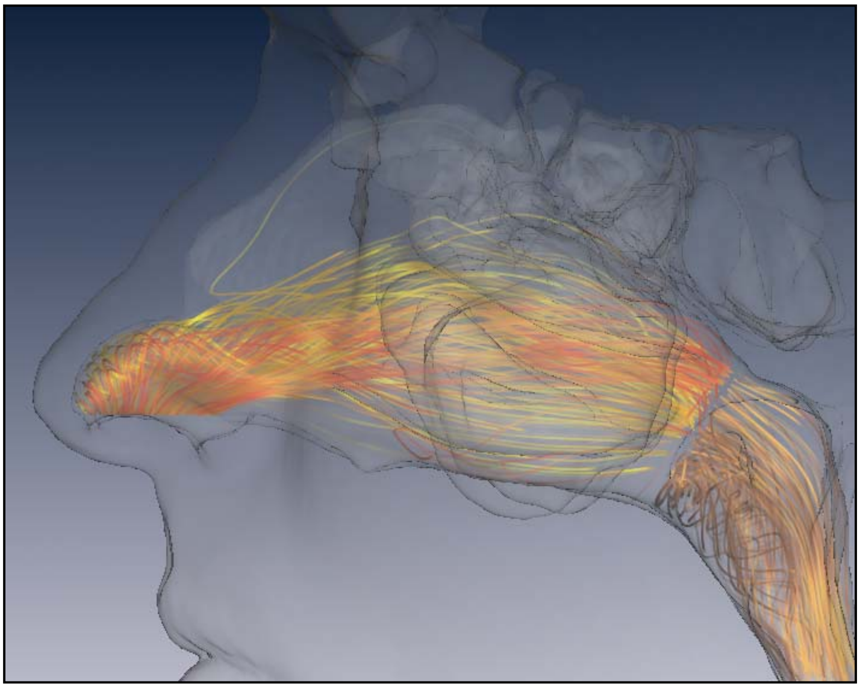

Illuminated streamline visualization of the velocity vector field with color coded discrimination of left (red) and right (gold) side

Therapy Planning in Rhinosurgery

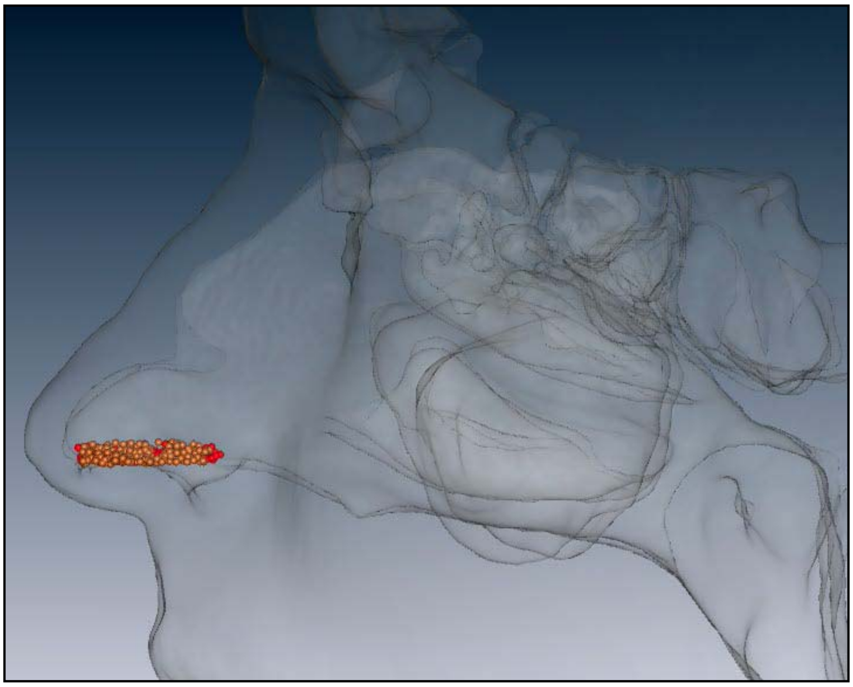

Inhalation: color coded discrimination of left (red) and right (gold) side

Therapy Planning in Rhinosurgery

Grid independence study (total flow rate)

- Coarse (0.9 MegaTets): tfr = 1398.6 cm^3/s
- Medium (1.6 MegaTets): tfr = 1440.3 cm^3/s
- Fine (2.2 MegaTets): tfr = 1491.3 cm^3/s
- Very fine (4 MegaTets): tfr = 1493.3 cm^3/s
- Super fine (8 MegaTets): tfr = 1494,1 cm^3/s

Validation (measurement vs. simulation)

- Rhinomanometry: difference < 5%
- Reproduction of left-right difference

Ansys CFX ®

Modifications of the Reference Model

- Reproduction of a hanging tip of the nose
- Reproduction of a tension nose
- Reproduction of a saddle nose
- Reproduction of a septal deviation

Work in Progress

- Assessment of pathological effects with regard to the regular airflow patterns

	unmodified	saddle	bump	hanging tip
velocity	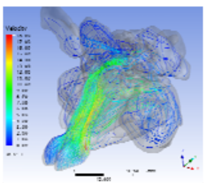	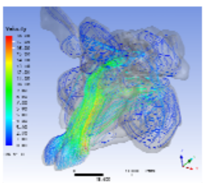	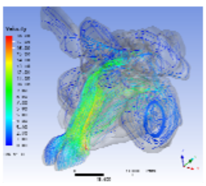	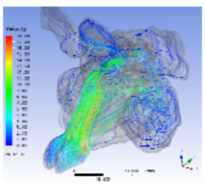
pressure	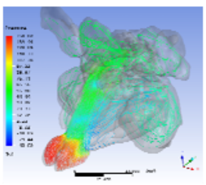	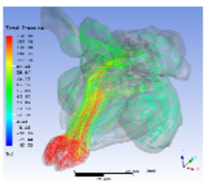	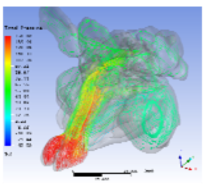	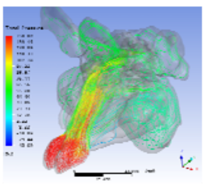
energy